Electroosmotic pumps and their applications in microfluidic systems

Xiayan Wang, **Chang Cheng**, **Shili Wang**, and **Shaorong Liu**
Department of Chemistry and Biochemistry, The University of Oklahoma, Norman, OK 73019, USA

Abstract

Electroosmotic pumping is receiving increasing attention in recent years owing to the rapid development in micro total analytical systems. Compared with other micropumps, electroosmotic pumps (EOPs) offer a number of advantages such as creation of constant pulse-free flows and elimination of moving parts. The flow rates and pumping pressures of EOPs matches well with micro analysis systems. The common materials and fabrication technologies make it readily integrateable with lab-on-a-chip devices. This paper reviews the recent progress on EOP fabrications and applications in order to promote the awareness of EOPs to researchers interested in using micro- and nano-fluidic devices. The pros and cons of EOPs are also discussed, which helps these researchers in designing and constructing their micro platforms.

Keywords

Electroosmosis; Micropump; Electroosmotic pump; Micro flow analysis

1 Introduction

Fluid pumping is an essential function of a microfluidic system and electroosmotic pumps (EOPs) are frequently utilized to perform this function. EOPs are developed based on electroosmosis, which is the movement of uncharged liquid relative to a stationary charged surface due to an externally applied electric field (Bockris and Reddy 1970). Electroosmosis is a phenomenon inherent to a solid—liquid interface (Hunter 1980). In 1809, Reuss (1809) discovered this phenomenon of electroosmosis, wherein the application of an electric field across a porous dielectric material caused liquid to flow. The interpretation of this phenomenon was accomplished by von Helmholtz (1879) using an electric double layer (EDL) model. Smoluchowski (1917) improved the Helmholtz theory after taking into account the actual distribution of ions in a capillary. The EDL theory has since served as the basis for interpretations of electrokinetic behaviors at liquid—solid interfaces. Electroosmosis has been used in capillary electrophoresis (CE) to drive buffer solution, often from anode to cathode, carrying both cations and anions to the detector for measurement. However, people usually do not consider this capillary (or the capillary system) to be an EOP. Therefore, EOPs in this format will not be discussed in this paper.

Electroosmotic pumps possess several outstanding features: EOPs are capable of generating constant and pulse-free flows, the flow magnitude and direction of an EOP are convenient to control, the pump can be fabricated using standard microfabrication technologies and thus is

readily integrateable with lab-on-chip (LOC) devices, and EOPs have no moving parts. EOPs have so far been used in various areas including high performance liquid chromatography (HPLC) separations (Pretorius et al. 1974; Chen et al. 2003a, 2004), LOC assays (Kutter et al. 1997; Li and Harrison 1997; Hadd et al. 1997), microelectronic equipment cooling (Jiang et al. 2002), drug delivery (Paul and Rakestraw 2000; Pikal 2001; Chen et al. 2007), device actuation (Paul and Rakestraw 2000), etc.

The majority of EOPs have been operated under a direct current (DC) voltage. These pumps are normally referred to as EOPs or DCEOPs. Due to electrolysis, bubbles will be produced at the electrodes, leading to serious problems if the electrodes are located inside a microfluidic channel. In order to eliminate bubbles formation, alternating current (AC) EOPs (or ACEOPs) are developed. This paper will cover both DCEOPs and ACEOPs. For those who are interested in other micropumps, they may check the references by Laser and Santiago (2004), Iverson and Garimella (2008) and Chen et al. (2008a) for more detailed information.

2 Theoretical aspect of electroosmotic pumping

2.1 DC electroosmotic pumping models

Electroosmosis requires charged solid surfaces to generate electroosmotic flow (EOF). Most surfaces spontaneously acquire a finite charge density when in contact with an aqueous solution. For example, a silica surface contacted with an aqueous solution becomes charged due to the deprotonation of the silanol groups on the surface. The charged surface attracts counterions and repels coions, resulting in the formation of an EDL. When an electric field is applied in parallel with the surface, cations in the EDL region are forced to move in the direction of the electric field. These mobile ions will drag the liquid, causing a net motion of the bulk fluid, as illustrated schematically in Fig. 1. The flow of the bulk fluid is the well-known EOF. Fluid propulsion devices based on EOF are generally called EOPs. EOPs are normally operated under a DC electric field. The materials utilized to create EOF are primarily open-channels or porous substances.

2.1.1 A model for open-channel electroosmotic pumps—In an open channel, the linear velocity (v_{eo}) of EOF can be evaluated by

$$v_{eo} = \frac{\varepsilon \zeta V}{4\pi \eta L},$$

(1)

where ε is the dielectric constant of the buffer solution, ζ is the zeta potential, V is the voltage applied across the channel, η is the viscosity constant of the pump solution, and L is the length of the pump channel (Liu et al.2003).

In an EOP system, a number of parallel pump channels may be used to increase flow rate. In the absence of external pressure, the EOF rate (Q_{eo}) can be expressed by

$$Q_{eo} = \frac{n \varepsilon \zeta V w d}{4\pi \eta L},$$

(2)

where w and d are the width and depth of the pump channel, and n is the number of the parallel channels. In this work we will use microfabricated pump channels as an example to describe the working principle of EOPs.

As an EOP is used to move the liquid in a fluidic network, a backpressure will be created. The fluidic network can often be replaced by an equivalent capillary with a diameter of d' and a length of L'. The magnitude of the backpressure can then be calculated using the Hagen—Poiseuille equation,

$$\Delta p = \frac{-128\eta L' Q_c}{\pi d'^4},$$
(3)

where Q_c is the flow rate in the equivalent capillary. The negative sign indicates that a pressure-driven flow is always from higher to lower pressure.

The backpressure also makes the solution in the pump channels flow backwards. Because the width of the pump channel is usually much greater than its depth, flow in such channels can be treated as flow in two parallel plates. The backward flow rate (Q_b) of n parallel pump channels can be described as (Bird et al. 2002):

$$Q_b = \frac{-nw\,(\Delta p)\,d^3}{12\eta L}.$$
(4)

Combination of Eqs. 3 and 4 gives,

$$Q_c = \frac{3\pi L d'^4 Q_b}{32 n L' w d^3}.$$
(5)

Because both Q_c and Q_b originate from Q_{eo}, and based on the incompressibility and continuity hypothesis of liquid fluids,

$$Q_{eo} = Q_c + Q_b.$$
(6)

Combination of Eqs. 2, 5 and 6 gives,

$$Q_c = \frac{3n\varepsilon\zeta V w d d'^4}{4\eta\,(3\pi L d'^4 + 32 n L' w d^3)}.$$
(7)

Equation 7 allows for the evaluation of flow rate in the fluidic network. It also provides valuable information guide in designing EOPs. For example, Q_c will always be directly proportional to ε, ζ and V. Q_c will increase with n, w and d directly proportionally when $d' \gg d$. If $d' \approx d$, Q_c will increase with n and w, but not at direct proportion.

In an EOP, the EOF is the only input flow, and it is split into a forward flow, Q_c, and a backward flow, Q_b. The efficiency of the pump, β, can be assessed by the ratio of Q_c (used to move the solutions in the fluidic network) to the total input flow Q_{eo},

$$\beta = \frac{Q_c}{Q_{eo}} = \frac{3\pi L d'^4}{3\pi L d'^4 + 32 n L' w d^3}.$$
(8)

From this equation, we see that the efficiency decreases as n, w or d increases, although the forward flow Q_c increases.

A similar model has been developed using round capillaries as pumping element. One may check the literature (Lazar and Karger 2002) for the related information.

2.1.2 A model for porous substance electroosmotic pumps—Porous substances have been utilized as pumping elements in EOPs. The interstitial spaces in the porous materials work like multiple flow passages in parallel with very small diameters. Zeng et al. (2001) have modeled the structure of a porous medium as an array of N capillaries with an effective radius of a, and a length of L_e—the tortuous flow path through the medium. For each of these capillaries, Rice and Whitehead's model (1965) can be used to evaluate the EOF in it.

$$v_z(r) = \frac{P_z}{4\eta}\left(a^2 - r^2\right) - \frac{\varepsilon\zeta E}{\eta}\left(1 - \frac{\phi(r/\lambda)}{\zeta}\right),$$

(9)

where $v_z(r)$ is the velocity profile, r is a variable representing the distance to the central axis of the capillary, P_z is the pressure gradient ($P_z = \Delta P/L_e$, where ΔP is the pressure drop across the capillary), E is the electric field strength ($E = V/L_e$, where V is the voltage applied), Φ is the potential in the capillary, λ is the double layer thickness, and ζ is the zeta potential.

Zeng et al. (2001) extended the analysis for an open capillary to that for a porous medium and obtained the flow rate of the entire porous medium

$$Q = -\frac{\Psi \Delta P A a^2}{8\eta L''\tau} - \frac{\Psi\varepsilon\zeta VA}{\eta L''\tau}\left(1 - \frac{2\lambda I_1(a/\lambda)}{aI_0(a/\lambda)}\right),$$

(10)

where Ψ is the porosity defined as the ratio of the void volume to the total volume of the porous medium, A is the cross-sectional area of the porous medium, τ stands for tortuosity [$\tau = (L_e/L'')^2$, where L'' is the physical length of the porous medium], I_0 is the zero-order modified Bessel function of the first kind, and I_1 is the first-order modified Bessel function of the first kind. By defining the maximum pressure ΔP_m as the ΔP at $Q = 0$ and the maximum flow rate Q_m as the Q at $\Delta P = 0$, we have

$$\Delta P_m = -\frac{8\varepsilon\zeta V}{a^2}\left(1 - \frac{2\lambda I_1(a/\lambda)}{aI_0(a/\lambda)}\right),$$

(11)

$$\text{and} \quad Q_m = -\frac{\Psi\zeta}{\tau}\frac{\varepsilon VA}{\eta L''}\left(1 - \frac{2\lambda_1(a/\lambda)}{aI_0(a/\lambda)}\right).$$

(12)

Combining Eqs. 11, 12 and 10, a linear relationship between the flow rate and the pressure of an EOP is obtained

$$Q = Q_m\left(1 - \frac{\Delta P}{\Delta P_m}\right).$$

(13)

The efficiency of an EOP can be estimated by

$$\beta = \frac{Q}{Q_m} = 1 - \frac{\Delta P}{\Delta P_m}$$

(14)

ΔP_m should be large in order to achieve a high EOP efficiency.

2.2 Working principle of AC electroosmotic pumps

DCEOPs are commonly operated under high electric fields. Potential issues associated with these pumps are bubble formation and reservoir pH variation due to electrolysis. ACEOPs are developed to address these issues, because application of an AC voltage does not result in any net electrolysis. In the last few years, it has been demonstrated that ACEOPs are capable of producing steady fluid flows (Ramos et al. 1999; Ajdari 2000; Brown et al. 2001), although the pumping power is low when compared with DCEOPs.

The working principle of ACEOPs was developed in the late 1990s and early 2000s. In 1999, Ramos et al. (1999) reported their observation of nonlinear electroosmotic flow resulting from the action of an AC field on a fluid. As an alternate voltage was applied to a pair of flat electrodes deposited on a glass slide, a steady electroosmotic flow, consisting of counter-rotating currents as shown in Fig. 2, was produced. Ramos et al. termed this phenomenon as AC electroosmosis (ACEO). However, these symmetrical electrodes produce only local flow circulation which are good for micro-mixers but cannot generate a net flow in the channel. In 2000, Ajdari (2000) theoretically predicted that a net ACEO flow can be created by using asymmetric electrodes. In 2001, Brown et al. (2001) experimentally validated this prediction and built the first ACEOP to pump water across an array of electrodes. Figure 3 presents a schematic diagram illustrating how a net ACEO flow is generated. As an AC voltage is applied between two asymmetric electrodes, a nonuniform electric field is created, leading to differential polarizations of ions near the electrodes. The movement of the net charges (excess ions) under the tangential component of the electric field induces a flow of the bulk solution, with a flow direction from the small electrode to the large electrode.

Net ACEO flows can be created using symmetric electrodes by applying a traveling-wave voltage to these electrodes (Cahill et al. 2004; Ramos et al. 2005; Garcia-Sanchez et al. 2006) or an AC voltage with a DC voltage offset (Wu 2008). The latter approach brings back the issues of DCEOPs due to the presence of the DC voltage which causes electrolysis. ACEO can also be produced by applying an AC voltage on electrodes with uneven thicknesses (a 3-dimensional structure) (see Fig. 4). Electroosmosis created in this fashion is called induced-charge electroosmosis (ICEO; Bazant and Ben 2006).

3 Electroosmotic pump fabrications techniques

In the above discussion, we have categorized EOPs into DCEOPs and ACEOPs. Based on the pumping elements used to generate EOP, DCEOPs can be further divided into open-channel, packed-column, porous-membrane and monolith EOPs. In the following sections, we will summarize the fabrication techniques according to these pump categories.

3.1 Fabrication of open-channel electroosmotic pumps

In open-channel EOPs, both narrow capillaries and micro-channels have been used as the pumping elements. Figure 5a presents a configuration of an open-capillary EOP (Dasgupta and Liu 1994). The pumping element of this EOP was a segment of a bare fused silica capillary (C1). A and B were two reservoirs holding a buffer (e.g. sodium tetraborate) solution. The reagent holding coil (HC) was a piece of capillary tubing filled with the reagent solution to be delivered. V1 was a selection valve. When the valve was set at the position as shown in Fig.

5a, the two syringes (S1 and S2) were isolated from the pump system. As the valve was switched to another position, S1 connected to C1 and S2 connected to HC. C1 could be rinsed with the solution in S1, and HC could be replenished with the reagent in S2. HV was a high-voltage power supply. A key component of this EOP is the grounding joint which separates the pumping element (C1) from the chemical reaction system (HC and the fluidic network after HC). It was constructed using a piece of Nafion ion exchange membrane tubing (M). Figure 5b presents a detailed construction of this joint. When C1 and connection capillary were joined, a small gap was left between them. Two PVC tubing sleeves were used to secure and seal M to C1 and the connection capillary. This membrane joint allowed electrical connectivity through ion conduction between the solutions inside and outside the membrane tubing, but solutions could not flow across the membrane. V1 was normally set to join the connection capillary and HC as exhibited in Fig. 5a. When a negative high voltage was applied, pump solution flows backwards, which allowed the free end capillary to aspirate solutions. When a positive high voltage was applied, pump solution flowed forward to propel the solutions in HC to the rest of the fluidic network.

The pump rate can be controlled by adjusting the electric field strength applied to C1. Alternatively, the pump rate can be boosted by employing parallel pumping capillaries. To construct a multiplexed-capillary EOP, an union is required to combine all the outlets of the capillaries into one outlet. Making such an union with small dead volumes was an issue for open-capillary EOPs (Liu and Dasgupta 1993,1994,1995). This issue can be easily addressed using microfabrication technologies.

Figure 6 presents an example of an open-channel EOP (Lazar and Karger 2002). The pumping element was a group of shallow microfabricated channels (1). All pumping channels had a common inlet (2) and outlet (3) reservoir. The pumping channels were exposed only to buffer solutions and did not come in contact with the sample solution. A porous glass disk (5 mm in diameter, 0.8–1 mm in width, and 4–5 nm pore size) was utilized to facilitate the electric field application between reservoirs 2 and 3, and also to prevent EOF leakage to reservoir 3. Reservoir 3 was fabricated from a PEEK external nut, and the porous glass disk was secured at the bottom of reservoir 3 with a corresponding internal nut. As a positive electric field was applied between reservoirs 2 and 3, EOF was generated to propel the downstream solution(s).

It is worth pointing out that the use of the porous glass disk in reservoir 3 had caused the electric current to drop within the first 10–15 min after the pump was turned on. This presents an issue for microfluidic applications if one cannot afford to wait for 10–15 min for the pump to "warm". The current drop was likely caused by the "ionenrichment and ion-depletion" effect as ionic species pass through nanometer-scale channels (Pu et al. 2004). This problem was alleviated when a low electric field was applied on the pumping channels (Lazar and Karger 2002). The above problem was solved by Takamura et al. (2001;2003) and Byun et al. (2007) who utilized polyacrylamide gels to make the electric connection and avoid EOF leakage.

Figure 7 illustrates the working principle of a cascade open-channel EOP (Takamura et al. 2001,2003). A cascade open-channel EOP uses low voltages to generate large EOFs. The pump shown in Fig. 8 is a three-stage cascade pump in which three groups of narrow pump channels (5 μm wide and 20 μm deep) were connected by two broad channels (50 μm wide and 20 μm deep). As an external voltage power supply was turned on, the same voltage was applied to each of the channel groups through a pair of gel electrodes, and EOF in all channels was moving downward. The EO flows in the two broad channels were "moving" against, but overpowered by those from the pump channels. The broad channels were wide so that little flow resistance was created against the EO flows of the pump channels. Since the pumping power was additive owing to the serial connection, the pumping pressure was tripled without increasing the voltage.

The pumping elements in open-channel EOPs were usually produced using standard photolithographic technologies (Chen and Santiago 2002; Pu and Liu 2004). Briefly, a glass wafer with a sacrificial layer of Cr and Au was spin-coated with a layer of photoresist and soft-baked. The photoresist was exposed to UV light under a mask aligner using the photomask containing the pump-channel pattern. Following the photoresist development, the exposed Au and Cr were etched off. The pump-channel pattern was etched into the glass water with HF. After the residual photoresist and Au and Cr layers were stripped off and access holes were drilled, the wafer was thermally bonded with a blank wafer to form an EOP device.

Using a photolithographic process, Morf et al. (2001) and Guenat et al. (2001) developed an EOP consisting of six parallel channels (each with a length of 83 mm, a width of 300 μm and a depth of 50 μm). Chen and Santiago (2002) constructed an EOP consisting of a short, wide and extremely shallow channel (with a length of 38 mm a width of 1 mm and a depth of 0.9 μm) incorporating eight equally distributed 0.25-mm wide ribs to improve the structural rigidity. Edwards et al. (2007) produced open-channel EOPs on chip consisting of multiple small channels (with 5-μm wide and 4-mm long channels) feeding into a larger flow channel (with 50 μm wide and 5 mm long). Typically, microfabricated EOPs can generate pressures of up to several atmospheres and flow rates of up to tens of μL per min.

Chemical derivatization has been used to modify the inner surface properties of the pumping channels for EOF generation, although virgin surfaces were used to create EO flows in most open-channel EOPs. In fact, surface modification creates another dimension for EOP designs. For example, a rapid field-free electroosmotic micropump (RFEP) was assembled with a Y-shaped pumping channel configuration (Joo et al. 2007). The surface of one Y arm was coated with a layer of an anionic polymer, and that of another was coated with a cationic polymer. Due to the opposite charges on the interior surfaces of these two arm channels, the EOFs flowed in opposite directions when an electric field was applied across these channels. A positive hydrodynamic pressure was developed at the common junction if both EOFs flowed into this joining point, while a negative pressure was induced when both EOFs flowed away from this point. The flow in the third channel responded rapidly and reversibly to the electric field on the other two channels.

3.2 Production of packed-column electroosmotic pumps

Packed-column EOPs have produced very high pressures (Paul et al. 1998). The basic methods for fabricating a packed EOP are similar to those for packed columns used in capillary electrochromatography. The pumping power will depend on the size of the particles packed. A pump pressure of more than 8,000 psi has been obtained using micron-size silica beads (Paul et al. 1998). Often, an increased pump pressure is obtained at a reduced flow rate, and vice versa. High flow rates are usually achieved using large particles (Paul and Rakestraw 2000). Zeng et al. (2001, 2002) prepared similar EO pumps by packing 3.5 μm diameter non-porous silica particles in fused silica capillaries with inner diameters ranging from 500 to 700 μm.

In order to generate high pressures while maintaining high flow rates, an EOP was constructed with parallel packed columns, three 20 cm × 530 μm i.d. fused silica capillaries packed with 20 ± 5 nm silica beads (Chen et al.2003a,b,2004,2005a). A flow rate of several μL/min and a pressure of over 20 MPa were achieved with an external voltage of 10 kV. Lately, Chen et al. (2008b) used nano-silica particles packed capillary to construct EOPs. They studied the pressure-flow rate characteristics of pump, the electric properties of the pump, and the influence of phosphate concentration on the pump.

Porous particles have also been packed into microfabricated channels. Borowsky et al. (2008a) constructed an EOP using a straight channel (3 cm × 160 μm × 62 μm) packed with

3.38 μm silica beads. The beads were held in place by a microfabricated weir structure. To reduce the effect of the pH change of a pump solution on the rate of an EOP, Razunguzwa and Timperman (2004) built an EOP consisting of two 500 μm channels with one packed with anion and the other packed with cation exchange beads. As the EOF rate from one channel increase due to the pH variations of the pump solution, the EOF rate from the other channel will decrease, and vice versa. Therefore, the overall EOF rate changes are thus (at least partially) offset. The pump built by Razunguzwa and Timperman (2004) could operate over a wide pH range (from 2 to 12).

3.3 Construction of porous-membrane electroosmotic pumps

A porous membrane contains many tortuous channels going from one side of the membrane to the other, and this material has been utilized to construct EOPs. Because the channels are relatively short, a high electric field strength is achieved when a low voltage is applied. Porous membranes, such as porous glass frit (Yao et al. 2003; Kim et al.2008), ion exchange membrane (Brask et al. 2005), silica membrane and alumina membrane (Prakash et al. 2006; Chen et al. 2008c) are commercially available. These materials can also be prepared in labs.

Using a porous core material produced from boric glass powder by high temperature sintering, Gan et al. (2000) built a porous-membrane EOP. The core had a diameter of 35 mm and a thickness of 13 mm. The average pore size ranged from 2 to 5 μm. The pump used low voltages (less than 500 V) and was capable of providing a wide flow rate range (10 μL/min—5.0 mL/min) under a moderate pressure (>0.15 MPa). Similar EOPs were also developed by Yao et al. (2001) using porous disc membranes. Other membrane materials made from silicon (Yao et al. 2003, 2006; Wallner et al. 2007), ion exchange membranes (Brask et al.2005), porous aluminum oxide (Miao et al. 2007; Prakash et al. 2006) and grafted porous polymer monolith (Tripp et al. 2004) have also been employed for EOP fabrications.

A porous-membrane EOP has the same configuration as one assembles a packed-column EOP. One can assemble a porous-membrane EOP the same way as does for a packed-column EOP. Because the membrane material is thin, it is advisable to use a supporting frame to secure the membrane and facilitate the fluidic and electric connections (Yao et al. 2003; Brask et al. 2005; Prakash et al. 2006; Yao et al. 2006).

3.4 Preparation of porous monolith electroosmotic pumps

Porous monolith EOPs utilize monolith columns as pumping elements. A porous monolith column is prepared by a polymerization process after the column is filled with a monomer, a crosslinker, a free radical initiator and a porogenic solvent. The monolith obtained is a single continuous piece of highly crosslinked porous polymer. An excellent feature of monolith columns is the elimination of frits which is usually used for packed-column EOPs. The monolithic materials used for EOP development can be either an organic polymeror an inorganic silica-monolith (Zou et al. 2002; Tanaka et al. 2002).

Chen et al. (2005a,b) prepared an EOP utilizing a solgel column with a length of 6 cm and an inner diameter of 100 μm. A piece of Nafion membrane was used to facilitate the electric connection. Similar EOPs were also produced by Wang et al. (2006). Using parallel, encased, monolithic silica capillary columns, Nie et al. (2007a) built EOPs on microchips, and implemented a two-line microchip flow injection analysis (Nie et al. 2007b). A problem with silica monoliths is that silica can be dissolved slowly in alkaline solutions. This dissolution will change the structure of the monolith and hence the EO pump rate. An organic polymer monolith can overcome this problem.

Detailed methods for making polymer monolith have been described in the literature (Peters et al. 1997; Lammerhofer et al. 2001). The following is a general protocol for making monoliths in a capillary. The inner wall of a capillary was first derivatized with 3-(trimethoxysilyl)propyl methacrylate. A polymerizing solution containing monomer, cross-linking reagent, progens and azo(bisisobutyronitrile) was then introduced into the capillary. This capillary, with both ends sealed by silicone septa, was submerged in a water bath at 55–60°C for polymerization for ~24 h. After the monolith was flushed with methanol to remove all unreacted components, a monolithic column was produced. The characteristic pore dimension of a monolith can be controlled over a broad range from 0.01 to 10 μm by altering the composition of the polymerization solution and the reaction temperature (Wang et al. 2006; Tripp et al. 2004; Xie et al. 2005; Aoki et al. 2006). The same protocol can be used to fabricate a monolith EOP in a microchip device. Attention should be paid to avoid void formation owing to the shrinking during polymerization. Too many of these voids could lead to variations of EO flow rates.

3.5 Manufacturing of AC electroosmotic pumps

Asymmetric electrodes are often utilized to generate ACEO flows in ACEOPs. The most common electrode design is an interdigitated asymmetric electrode assembly, although a number of other layouts have been tested. Usually, metal electrodes are deposited onto a substrate by sputtering or chemical vapor deposition. The electrode materials include gold—Nichrome (Brown et al. 2001), platinum—titanium (Studer et al. 2004), gold—chromium (Debesset et al. 2004), titanium—gold—titanium (Garcia-Sanchez et al. 2006), indium tin oxide (ITO) (Mpholo et al.2003), etc. These electrodes are normally fabricated in a planar format (with the same thickness).

Electrodes of alternating thicknesses have recently been examined by Bazant's group (Bazant and Ben 2006; Urbanski et al. 2006, 2007) to promote the pump rates of ACEOPs. The fabrication process includes a deposition of an array of interdigitated electrodes on a substrate followed by electroplating a subset of the electrodes to increase their thickness.

Table 1 summarizes the performance metrics reported for the various EOPs.

4 Electroosmotic pump applications

ACEOP is a developing area of research. Although it has received much attention in recent years, papers of ACEOPs for real applications have not been found. Almost all studies have focused on the theoretical models, numerical analysis, and experimental demonstration. So, in this section we only focus on the application of DCEOPs.

4.1 Micro flow injection analysis (*μ*-FIA)

One of the earliest applications of EOP was in FI analysis by Liu and Dasgupta (1992). The EOP system employed for FIA resembled a capillary electrophoresis setup, and consisted of a capillary, an on-capillary absorbance detector and a high-voltage power supply. The capillary was pre-filled with a reagent (1,10-phenanthroline) solution, and its ends were immersed in two vials containing the reagent solution. Samples (Fe^{2+}) were introduced by moving the sampling end of the capillary into a sample valve via a hydrodynamic injection scheme (identical to that in capillary electrophoresis). After sample injection, the sampling end of the capillary was moved back to the reagent vial and a voltage was applied across the capillary to carry out the analysis. The chemical reaction was preceded as Fe^{2+} electrophoretically migrated into the reagent zone, and the product was brought to the detector by both electrophoretic migration and electroosmotic flow. Fe^{2+} samples within 5–200 mg/L were analyzed using this method, and a relative standard deviation of 2.9% was obtained. The major contribution of the standard deviation was from the sampling errors.

To decrease the sampling errors, the same authors incorporated a 100-nL volumetric injection valve near the sampling end of the capillary in their system (Liu and Dasgupta 1993), and demonstrated a combination of electrophoretic separation and flow analysis in a single-line FI setup for multi-analyte determinations. The carrier stream contained 2-pyridyl(azoresorcinol) as the chromogenic reagent and 10 mM NBu_4ClO_4 as the background electrolyte. A mixture of five metal ions (Co^{2+}, Ni^{2+}, Zn^{2+}, Cd^{2+} and Sm^{3+}) was injected into a fused silica capillary via the electrically nonconducting injection valve. When an electric field was applied, the metal ions migrated forward to react with the chelating reagent, forming chelated metal ion complexes. As the complexes were electrophoretically and electroosmotically driven to the detector, they were separated. The large cation, NBu_4^+ in the background electrolyte solution was used to match the mobility of the chelated metal ion complexes so as to minimize the dispersion of the product bands.

It is well known that a single-line FI system will distort the product peak (Ruzicka and Hansen 1981), especially when the sample plug is long, and a multi-line FI system is often selected to eliminate this problem. To demonstrate EOPs for multi-line FI applications, Dasgupta and Liu (1994) constructed a two-line FI system for chloride determination. Referring to Fig. 8, there were two EOPs similar to that described in Fig. 5, but each pump consisted of four single open capillary (40 cm × 75 μm i.d. × 375 μm o.d.) pumps in order to increase the flow rate. The pump electrolyte (2 mM sodium tetraborate) was directly used as the carrier stream in which the sample was injected via V2 (100 nL injection volume) and, therefore, a holding coil was not necessary in this line. A holding coil, HC, was used in the reagent [0.8 mM $Hg(SCN)_2$ and 0.2 M $Fe(NO_3)_3$] line. The chemistry behind this method involved a reaction between chloride and mercuric thiocyanate, forming mercuric chloride and releasing thiocyanate. The released thiocyanate reacted with ferric ion in the same solution, forming a blood-red complex which could be detected by an absorbance detector. In this system, the flow rate of each pump was ~1.7 μL/min. Good linear relationship was obtained for Cl⁻ determination [$R^2 = 0.996$ for 50–600 ppm (Cl⁻)], with a relative standard deviation of ≤0.8% ($n = 13$).

A similar EOP has also been used for SI analysis of nitrite-nitrogen and ammonia-nitrogen (Liu and Dasgupta 1994). Figure 9 presents the configuration of the SI system. The HC is a capillary holding coil with a length of 40 cm and an inner diameter of 250 μm. The EOP was connected to the common port of a selection valve (V2) which was pneumatically operated. The Griess—Saltzman reactions (Griess 1879) were employed for nitrite-nitrogen analysis and the nitroprusside-catalyzed Berthelot reaction (Berthelot 1859) was utilized for ammonia-nitrogen determinations. This application took advantage of an EOP capable of instant flow direction switching. Excellent linear relationships ($R^2 = 1.000$) were obtained for both nitrite-nitrogen (20–400 μm) and ammonia-nitrogen (50–600 μm). The same system was further incorporated with a miniaturized diffusion scrubber (Liu and Dasgupta 1995) or a droplet sampler (Yang et al. 2001) for gaseous ammonia monitoring.

Gan et al. (2000) developed an EO pump SI system to determine Cr(VI) in waste water. The pump rate increased linearly with the applied voltage from 100 to 500 V. At 500 V, the pump rate was ~3 mL/min. Two EOPs and an 8-way selection valve were employed to build the SI system. Up to 7.0 mg/L Cr(VI) was analyzed with a relative standard deviation of 0.4%. Yang et al. (2001) introduced an electrokinetic flow analytical system using an EOP and a bi-directional electrostacking unit for determination of Cr(VI) and Pb(II) in drinking water. Graphite furnace atomic absorption spectrometry was used as the detector. Good linear relationships were obtained for both of Cr(VI) and Pb(II) from 0.2 to 40 μg/L. The detection limit was 10 ng/L for Cr(VI) and 13 ng/L for Pb(II). The recovery was 103–105% for Cr(VI) and 95.9–96.9% for Pb(II). Zhao et al. (2002) reported an EO pumped SI method for nitrite-nitrogen determination. The system consisted of an EOP, two solenoid valves and an absorbance detector. The method was based on the Griess—Saltzman reactions (Griess

1879; Saltzman 1954) to form a colored product which was measured at 540 nm. A linear calibration curve was obtained for nitrite-nitrogen from 10–800 μg/L, with a detection limit of 1 μg/L. Chen et al. (2005c) constructed a μ-FI system that integrated a monolithic EOP, a micro injector and a microchip electrochemical detector on a single microchip for dopamine measurement.

Pu and Liu (2004) manufactured an EOP on a microchip and demonstrated its application for an enzyme inhibition assay. Figure 10a shows the photomask design of the pump chip and Fig. 10b exhibits the schematic arrangement of the SI system. The microchip EOP contained a pumping element of 32 parallel channels, each with a depth of 20 μm and a total length of ~27 cm. An isolation channel was also fabricated on the chip to separate the sample/reagent solutions from the pumping solution. The isolation channel served as a sample/reagent holding coil as well for the SI analysis. The experimental setup was identical to a conventional SI system except for the microchip EOP. The system was applied to β-Galactosidase-catalyzed hydrolysis of fluorescein di(β-ᴅ-galactoside) and inhibition of this hydrolysis reaction by diethylenetriaminepentaacetic acid. There were three basic steps to accomplish the assay. Step 1, a negative high voltage was applied to the EOP to aspirate sample and reagents into the isolation channel. Step 2, after the sample and reagents were reacted adequately, a positive high voltage was applied to the pump to propel the product to the detector for measurement. Step 3, the system was reset (this included washing the sampling capillary attached to the selection valve and loading this capillary with the next sample solution).

4.2 Microfluidic liquid chromatography systems (μ-LC)

Electroosmotic pumps offer a simple and cost-effective means to produce adequate pressures and flow rates for capillary chromatographic separation. Paul et al. (2000) constructed a capillary HPLC using packed-column EOPs for separations of polycyclic aromatic hydrocarbons. Chen et al. (2003a, 2004) built an EOP capable of generating pressures in excess of 3 MPa and flow rates in the range of μL/min. The pump consisted of three parallel fused silica capillary columns (25 cm × 530 μm i.d.) packed with 2 μm silica beads. Hollow metal tubings were used as grounding electrodes. To characterize the EOP, a pressure transducer was utilized to measure the pumping pressures. Figure 11 presents a schematic diagram of the one-stage EOP and the μ-HPLC system (Chen et al. 2004). The μ-HPLC system consisted of a four-port injection valve with a internal loop of 200 nL, 15 cm × 320 μm i.d. 5 μm Spherigel C_{18} stainless steel analytical column and a on-column UV—Vis detector. To evaluate the performance of the system, a mixture of thiourea, benzene, toluene, naphthalene, phenanthrene, biphenyl and anthracene were separated. Acetonitrile/water was used as their mobile phase. The number of theoretical plates of the column was 2.3–3.2×10^4/m using the EOP, and 1.4–2.3×10^4/m using a mechanical pump. The error of retention time (t_r) expressed in RSD% was within 0.8% with the EOP for all compounds tested, while the error of t_r was 3.6% with the mechanical pump.

Electroosmotic pumps were also used by Reichmuth and Kirby (2003) for reversed phase HPLC separations. With this system, the authors investigated the effects of ammo-nioalkyl sulfonate additives on electrokinetic pumping and separation. A gradient solvent delivery system was developed by Figeys and Aebersold (1998) using two open-channel EOPs. One pump was used to pump an aqueous solvent and the other for organic solvent, and a gradient solvent was produced by varying the pump rates. The solvent delivery system was integrated with a reverse phase microcolumn and an electrospray ionization ion trap mass spectrometer for peptide analysis. A concentration limit of detection of 100 amol/μL was achieved.

Lazar et al. (2006) developed a microchip HPLC system (Fig. 12) for proteomic investigations. The microchip integrated all the necessary functional components (e.g. pump, valve, separation column, and electrospray interface) for LC—MS analysis. The overall size of the microfluidic

network was so small that two fully functional HPLC systems can be incorporated on a 7.62 cm × 2.54 cm glass chip. The device was tested for analysis of protein digests obtained from the MCF7 breast cancer cell line. The analysis enabled confident identifications of 77 proteins, demonstrated that these chips can be used for high-throughput biomarker discovery.

Very recently, a microchip LC system integrated with EOP was reported to separate six nitroaromatic and nitramine explosives and their degradation products (Borowsky et al. 2008b). The pump and LC channels were fabricated on a single quartz substrate. The pump was a channel (3.0 cm × 230 μm × 100 μm) packed with 5-μm porous silica particles, and the separation column was a channel (2.6 cm × 230 μm 9 100 μm) with phenethyl sol-gel monolith stationary phase.

4.3 Microreactors

Jin et al. (2003) reported a microchamber reactor on microchip used as proteolytic digestion system driven by electroosmotic pumping. Digestions of proteins in the EOF-driven microchamber were subsequently carried out for 12 min, and the tryptic peptides were analyzed independently using capillary electrophoresis (CE) and MALDITOF mass spectrometry (MS). The results from CE analysis of the tryptic peptides from the EOF-driven proteolytic system and a conventional water bath digestion (18 h water bath digestion at 37°C) were comparable.

4.4 Micro energy systems

Electroosmotic pumps have been used in micro energy systems, as well. Santiago's group has proposed a number of applications of EOPs for miniature cells: active water management in proton exchange membrane (PEM) fuel cells, methanol/water mixture delivery in direct methanol fuel cells (DMFCs) and air delivery/displacement in PEM fuel cells via liquid EO pumping.

Water management is a significant challenge in portable fuel cells and particularly in fuel cells with air-breathing cathodes. Water flooding at the cathode of a fuel cell is a common problem in fuel cells. Excessive flooding of the open cathode can lead to a dramatic reduction of fuel cell power. Buie et al. (2006a) developed proton exchange membrane fuel cells with integrated planar electroosmotic pumping structures that actively removed liquid water from cathode flow channels. EOPs have no moving parts, scale appropriately with fuel cells, operate across a wide range of conditions, and consume a small fraction of fuel cell power. EOPs can relieve cathode design barriers and simplify water management in fuel cells. In their system, two 1.1-mm thick porous glass EOPs, spaced 2 mm apart, made up the walls of the cathode channel. The results showed that removing water from the cathode using integrated EO pumping structures improved fuel cell performance and stability.

Fabian et al. (2006) designed a water management system in which the water was driven by an EOP. A hydrophilic conductive wick was in direct contact with cathode gas diffusion layer and served as a water collector layer that hydraulically linked the entire cathode surface with the EOP located outside of the fuel cell assembly. The prototype air-breathing fuel cell with this water management design successfully functioned under severe flooding conditions, including ambient temperature 10°C and relative humidity 80%, for up to 6 h without any observable cathode flooding or loss of performance.

Litster et al. (2007) incorporated an EOP into a larger 25 cm^2 PEM fuel cell as an active water management system. The pumping element of the EOP was a 2 cm^2 borosilicate frit with a thickness of 1 mm, a mean pore diameter of 2 μm and a porosity of 40%. The EOP prevented flooding and provided rapid recovery from severe flooding. With this EOP, a 25 cm^2 fuel cell was able to operate at an air stoichiometry of 1.3 while maintaining a power density of 0.42

W/cm^2. It was 60% greater than the maximum power density achievable with a nonporous flow field under the same conditions.

Except for water removal from cathodes of fuel cells, EOPs have also been used as a driving force for fuel delivery. Kim et al. (2006) reported the utilization of a porous-membrane EOP to pump methanol/water. The power consumption of the EOP was about 2% of the direct methanol fuel cell power generation, assuming that the unit cell operates at 0.4 V to produce 200 mA/cm^2, the fuel cell area was the same as the pump area, and fuel utilization was 100% with 1 mol/L methanol feed. Buie et al. (2006b) developed a miniature-free convection DMFC that utilized an EOP for methanol delivery.

4.5 Microelectronic cooling systems

Electroosmotic pumps have been used for electronic device cooling, as well. The rapid increase in power density and total power of microelectronics has spurred interest in miniaturized cooling systems that can achieve high heat dissipation rates. A compact micropump is therefore a vital component for the high efficiency cooling of integrated Microsystems. EOPs, having no moving structural elements, have received much recent attention because of the potential of achieving both high pressure and large flowrate.

Yao et al. (2001) developed high flowrate EOP designed for microcooling applications. The EOPs were fabricated using modified commercially available sintered-glass frits. The frits were porous cylinders 30 mm in diameter and 1.5–3 thick and provided the high wetted-surface-to-volume ratio required to generate pressures exceeding 2 atm. Both deionized water and buffered aqueous solutions have been used as working fluids. The prototype pumps demonstrated a flowrate of 7 mL/min for 200 V applied potential that is suitable for two-phase heat exchangers with a capacity approaching 100 W.

Jiang et al. (2002) built a closed-loop cooling system using two-phase microchannel heat sink and electroosmotic pumping for applications in VLSI chips cooling. The silicon heat exchanger attached to the test chip (1 cm^2) achieved junction-fluid resistance near 0.1 K/W using 40 plasma-etched channels with hydraulic diameter of 100 μm. The EOP, made of an ultrafine porous glass frit with working volume of 1.4 cm^3, achieved maximum backpressure and flowrate of 160 KPa and 7 mL/min, respectively, using 1 mM buffered de-ionized water as working fluid. The closed-loop system removed 38 W with pump power of 2 W and junction-ambient thermal resistance near 2.5 K/W.

5 Conclusions

Electroosmotic pumps have been demonstrated to be efficient for fluid propulsion in microfluidic systems. EOPs are capable of producing flows at high pump rates and against high backpressures. Often, high pump rates are obtained at low pump pressures, and vice versa. This should not be an issue, because typically a high flow rate FI/SI system has relatively low flow resistance, unless a packed bed reactor or a filtration system is used. The most important features of an EOP are that it has no moving parts, generates pulse-free and stable flows, and are readily integratable with microfluidic and MEMS devices. EOF pumps happen to be ideally suited for microfluidic systems in which pulse-free and stable flow is desired.

The robustness and reliability of EOPs have been a concern in some applications. When different solutions pass through an EOP, its pump rate may change because of the adsorption of compounds from the samples/sample matrix onto the surfaces of the pumping elements. This problem can be eliminated by isolating the pump fluid from the sample/reagent solutions in the analytical system. When properly designed, EOPs can be used as a stand-alone pump or

integrated into a microchip device to generate adequate flow rates and pressures for miniaturized HPLC development.

Acknowledgments

References

Ajdari A. Pumping liquids using asymmetric electrode arrays. Phys Rev E 2000;61(1):R45–R48.

Aoki H, Kubo T, Ikegami T, Tanaka N, Hosoya K, Tokuda D, Ishizuka N. Preparation of glycerol dimethacrylate-based polymer monolith with unusual porous properties achieved via viscoelastic phase separation induced by monodisperse ultra high molecular weight poly(styrene) as a porogen. J Chromatogr A 2006;1119(1–2):66–79. [PubMed: 16513125]

Bazant MZ, Ben Y. Theoretical prediction of fast 3D AC electro-osmotic pumps. Lab Chip 2006;6(11): 1455–1461. [PubMed: 17066170]

Berrouche Y, Avenas Y, Schaeffer C, Wang P, Chang H-C. Optimization of high flow rate nanoporous electroosmotic pump. J Fluids Eng 2008;130(8):081604/1–081604/6.

Berthelot M. Violet d'aniline. Rep Chim Appl 1859;1:284.

Bird, RB.; Stewart, WE.; Lightfoot, EN. Transport phenomena. 2nd edn. Wiley Interscience; New York: 2002.

Bockris, JO'M.; Reddy, AKN. Modern electrochemistry. Vol. vol 2. Plenum Press; New York: 1970. p. 826-835.

Borowsky J, Lu Q, Collins GE. High pressure electroosmotic based on a packed bed planar microchip. Sens Actuat B Chem 2008a;131(1):333–339.

Borowsky JF, Giordano BC, Lu Q, Terray A, Collins GE. Electroosmotic flow-based pump for liquid chromatography on a planar microchip. Anal Chem 2008b;80(21):8287–8292. [PubMed: 18837518]

Brask A, Kutter JP, Bruus H. Long-term stable electroosmotic pump with ion exchange membranes. Lab Chip 2005;5(7):730–738. [PubMed: 15970966]

Brown ABD, Smith CG, Rennie AR. Pumping of water with ac electric fields applied to asymmetric pairs of microelectrodes. Phys Rev E 2001;63(1–2):016305/1–016305/8.

Buie CR, Posner JD, Fabian T, Cha SW, Kim D, Prinz FB, Eaton JK, Santiago JG. Water management in proton exchange membrane fuel cells using integrated electroosmotic pumping. J Power Sources 2006a;161(1):191–202.

Buie CR, Kim D, Litster SE, Santiago JG. Free convection direct methanol fuel cells powered by electroosmotic pumps. ECS Trans 2006b;3(1):1279–1287.

Byun CK, Wang X, Pu Q, Liu S. Electroosmosis-based nanopipettor. Anal Chem 2007;79(10):3862–3866. [PubMed: 17428033]

Cahill BP, Heyderman LJ, Gobrecht J, Stemmer A. Electro-osmotic streaming on application of traveling-wave electric fields. Phys Rev E 2004;70(3–2):036305-1–14.

Chen CH, Santiago JG. A planar electroosmotic micropump. J Microelectromech Syst 2002;11(6):672–683.

Chen L, Ma J, Guan Y. An electroosmotic pump for packed capillary liquid chromatography. Microchem J 2003a;75(1):15–21.

Chen L, Ma J, Tan F, Guan Y. Generating high-pressure submicroliter flow rate in packed microchannel by electroosmotic force: potential application in microfluidic systems. Sens Actuat B Chem 2003b; 88(3):260–265.

Chen L, Ma J, Guan Y. Study of an electroosmotic pump for liquid delivery and its application in capillary column liquid chromatography. J Chromatogr A 2004;1028(2):219–226. [PubMed: 14989475]

Chen L, Guan Y, Ma J, Luo G, Liu K. Application of a high-pressure electro-osmotic pump using nanometer silica in capillary liquid chromatography. J Chromatogr A 2005a;1064(1):19–24. [PubMed: 15729816]

Chen L, Wang H, Ma J, Wang C, Guan Y. Fabrication and characterization of a multi-stage electroosmotic pump for liquid delivery. Sens Actuat B Chem 2005b;104(1):117–123.

Chen Z, Wang P, Chang HC. An electro-osmotic micro-pump based on monolithic silica for micro-flow analyses and electro-sprays. Anal Bioanal Chem 2005c;382(3):817–824. [PubMed: 15803307]

Chen L, Choo J, Yan B. The microfabricated electrokinetic pump: a potential promising drug delivery technique. Export Opin Drug Deliv 2007;4(2):119–129.

Chen L, Lee S, Choo J, Lee EK. Continuous dynamic flow micropumps for microfluid manipulation. J Micromech Microeng 2008a;18(1):013001/1–013001/22.

Chen L, Li Q, Lee S, Choo J. Development of an electro-osmotic pump using nanosilica particle packed capillary. IEEE Sens J 2008b;8(5):488–494.

Chen YF, Li MC, Hu YH, Chang WJ, Wang CC. Low-voltage electroosmotic pumping using porous anodic alumina membranes. Microfluid Nanofluid 2008c;5(2):235–244.

Dasgupta PK, Liu S. Electroosmosis: a reliable fluid propulsion system for flow injection analysis. Anal Chem 1994;66(11):1792–1798.

Debesset S, Hayden CJ, Dalton C, Eijkel JCT, Manz A. An AC electroosmotic micropump for circular chromatographic applications. Lab Chip 2004;4(4):396–400. [PubMed: 15269811]

Edwards JMIV, Hamblin MN, Fuentes HV, Peeni BA, Lee ML, Woolley AT, Hawkins AR. Thin film electro-osmotic pumps for biomicrofluidic applications. Biomicrofluidics 2007;1(1):014101/1–014101/11.

Fabian T, O'Hayre R, Litster S, Prinz FB, Santiago JG. Water management at the cathode of a planar air-breathing fuel cell with an electroosmotic pump. ECS Trans 2006;3(1):949–960.

Figeys D, Aebersold R. Nanoflow solvent gradient delivery from a microfabricated device for protein identifications by electrospray ionization mass spectrometry. Anal Chem 1998;70(18):3721–3727. [PubMed: 9751016]

Gan W, Yang L, He Y, Zeng R, Cervera ML, de la Guardia M. Mechanism of porous core electroosmotic pump flow injection system and its application to determination of chromium(VI) in waste-water. Talanta 2000;51(4):667–675. [PubMed: 18967898]

Garcia-Sanchez P, Ramos A, Green NG, Morgan H. Experiments on ac electrokinetic pumping of liquids using arrays of microelectrodes. IEEE Trans Electr Insul 2006;13(3):670–677.

Griess JP. Ber Deutsch Chem Ges 1879;12:426.

Guenat OT, Ghiglione D, Morf WE, de Rooij NF. Partial electroosmotic pumping in complex capillary systems. Part 2: Fabrication and application of a micro total analysis system (µTAS) suited for continuous volumetric nanotitrations. Sens Actuat B Chem 2001;72(3):273–282.

Hadd AG, Raymond DE, Halliwell JW, Jacobson SC, Ramsey JM. Microchip device for performing enzyme assays. Anal Chem 1997;69(17):3407–3412. [PubMed: 9286159]

Helmholtz von HLF. Studien uber electrische grenzschichten. Ann Phys 1879;7:337–382.

Hunter, RJ. Comprehensive treatise of electrochemistry. Brockris, JO'M.; Conway, BE.; Yeager, E., editors. Vol. vol 1. Plenum Press; New York: 1980. p. 404-412.

Iverson BD, Garimella SV. Recent advances in microscale pumping technologies: a review and evaluation. Microfluid Nanofluid 2008;5(2):145–174.

Jiang L, Mikkelsen J, Koo JM, Huber D, Yao S, Zhang L, Zhou P, Maveety JG, Prasher R, Santiago JG, Kenny TW, Goodson KE. Closed-loop electroosmotic microchannel cooling system for VLSI circuits. IEEE Trans Comp Pack Manuf Technol 2002;25(3):347–355.

Jin LJ, Ferrance J, Sanders JC, Landers JP. A microchip-based proteolytic digestion system driven by electroosmotic pumping. Lab Chip 2003;3(1):11–18. [PubMed: 15100799]

Joo S, Chung TD, Kim HC. A rapid field-free electroosmotic micropump incorporating charged microchannel surfaces. Sens Actuat B Chem 2007;123(2):1161–1168.

Kim D, Posner JD, Santiago JG. Electroosmotic pumping of methanol/water mixtures for direct methanol fuel cell applications. ECS Trans 2006;1(6):241–245.

Kim D, Posner JD, Santiago JG. High flow rate per power electroosmotic pumping using low ion density solvents. Sens Actuat A 2008;141(1):201–212.

Kutter JP, Jacobson SC, Ramsey JM. Integrated microchip device with electrokinetically controlled solvent mixing for isocratic and gradient elution in micellar electrokinetic chromatography. Anal Chem 1997;69(24):5165–5171.

Lammerhofer M, Svec F, Frechet JMJ, Lindner W. Capillary electrochromatography in anion-exchange and normal-phase mode using monolithic stationary phases. J Chromatogr A 2001;925(1–2):265–277. [PubMed: 11519811]

Laser DJ, Santiago JG. A review of micropumps. J Micromech Microeng 2004;14(6):R35–R64.

Lastochkin D, Zhou R, Wang P, Ben Y, Chang HC. Electrokinetic micropump and micromixer design based on ac faradaic polarization. J Appl Phys 2004;96(3):1730–1733.

Lazar LM, Karger BL. Multiple open-channel electroosmotic pumping system for microfluidic sample handling. Anal Chem 2002;74(24):6259–6268. [PubMed: 12510747]

Lazar IM, Trisiripisal P, Sarvaiya HA. Microfluidic liquid chromatography system for proteomic applications and bio-marker screening. Anal Chem 2006;78(15):5513–5524. [PubMed: 16878890]

Li PCH, Harrison DJ. Transport, manipulation, and reaction of biological cells on-chip using electrokinetic effects. Anal Chem 1997;69(8):1564–1568. [PubMed: 9109354]

Litster S, Buie CR, Fabian T, Eaton JK, Santiago JG. Active water management for PEM fuel cells. J Electrochem Soc 2007;154(10):B1049–B1058.

Liu S, Dasgupta PK. Flow injection analysis in the capillary format using electroosmotic pumping. Anal Chim Acta 1992;268(1):1–6.

Liu S, Dasgupta PK. A simple means to increase absorbance detection sensitivity in capillary zone electrophoresis. Anal Chim Acta 1993;283(2):747–753.

Liu S, Dasgupta PK. Sequential injection analysis in capillary format with an electroosmotic pump. Talanta 1994;41(11):1903–1910. [PubMed: 18966148]

Liu S, Dasgupta PK. Electroosmotically pumped capillary format sequential injection analysis with a membrane sampling interface for gaseous analytes. Anal Chim Acta 1995;308(1–3):281–285.

Liu S, Pu Q, Lu JJ. Electric field-decoupled electroosmotic pump for microfluidic devices. J Chromatogr A 2003;1013(1–2):57–64. [PubMed: 14604108]

Miao J, Xu Z, Zhang X, Wang N, Yang Z, Sheng P. Micropumps based on the enhanced electroosmotic effect of aluminum oxide membranes. Adv Mater 2007;19(23):4234–4237.

Morf WE, Guenat OT, de Rooij NF. Partial electroosmotic pumping in complex capillary systems. Part 1: Principles and general theoretical approach. Sens Actuat B Chem 2001;72(3):266–272.

Mpholo M, Smith CG, Brown ABD. Low voltage plug flow pumping using anisotropic electrode arrays. Sens Actuat B Chem 2003;92(3):262–268.

Nie F, Macka M, Barron L, Connolly D, Kent N, Paull B. Robust monolithic silica-based on-chip electro-osmotic micro-pump. Analyst 2007a;132(5):417–424. [PubMed: 17471387]

Nie F, Macka M, Paull B. Micro-flow injection analysis system: on-chip sample preconcentration, injection and delivery using coupled monolithic electroosmotic pumps. Lab Chip 2007b;7(11):1597–1599. [PubMed: 17960291]

Peters EC, Petro M, Svec F, Frechet JMJ. Molded rigid polymer monoliths as separation media for capillary electro-chromatography. Anal Chem 1997;69(17):3646–3649. [PubMed: 9286168]

Paul, PH.; Arnold, DW.; Rakestraw, DJ. Electrokinetic generation of high pressures using porous microstructures. In: Harrison, DJ.; van den Berg, A., editors. Micro total analysis system. Springer; New York: 1998. p. 49-52.

Paul, PH.; Rakestraw, DJ. Electrokinetic high pressure hydraulic system. US Patent. 6,019,882. 2000.

Paul, PH.; Arnold, DW.; Neyer, DW.; Smith, KB. Electrokinetic pump application in micro-total analysis systems: mechanical actuation to HPLC. In: Harrison, DJ.; van den Berg, A., editors. Micro total analysis system. Springer; New York: 2000. p. 583-590.

Pikal MJ. The role of electroosmotic flow in transdermal iontophoresis. Adv Drug Deliv Rev 2001;46(1–3):281–305. [PubMed: 11259844]

Prakash P, Grissom MD, Rahn CD, Zydney AL. Development of an electroosmotic pump for high performance actuation. J Membr Sci 2006;286(12):153–160.

Pretorius V, Hopkins BJ, Schieke JD. Electroosmosis. New concept for high speed liquid chromatography. J Chromatogr A 1974;99:23–30.

Pu Q, Liu S. Microfabricated electroosmotic pump for capillary-based sequential injection analysis. Anal Chim Acta 2004;511(1):105–112.

Pu Q, Yun J, Temkin H, Liu S. Ion-enrichment and ion-depletion effect of nanochannel structures. Nano Lett 2004;4(6):1099–1103.

Ramos A, Morgan H, Green NG, Castellanos A. AC electric-field-induced fluid flow in microelectrodes. J Colloid Interf Sci 1999;217(2):420–422.

Ramos A, Gonzalez A, Castellanos A, Green NG, Morgan H. Pumping of liquids with ac voltages applied to asymmetric pairs of microelectrodes. Phys Rev E 2003;67(5–2):056302/1–056302/11.

Ramos A, Morgan H, Green NG, Castellanos A. Pumping of liquids with traveling-wave electroosmosis. J Appl Phys 2005;97(8):084906/1–084906/8.

Razunguzwa TT, Timperman AT. Fabrication and characterization of a fritless microfabricated electroosmotic pump with reduced pH dependence. Anal Chem 2004;76(5):1336–1341. [PubMed: 14987090]

Reichmuth DS, Kirby BJ. Effects of ammonioalkyl sulfonate internal salts on electrokinetic micropump performance and reversed-phase HPLC separations. J Chromatogr A 2003;1013(1–2):93–101. [PubMed: 14604111]

Reuss FF. Sur un nouvel effet de l'électricité galvanique. Mémoires de la Société Impériale des Naturalistes de Moscou 1809;2:327–337.

Rice CL, Whitehead R. Electrokinetic flow in a narrow cylindrical capillary. J Phys Chem 1965;69(11):4017–4024.

Ruzicka, J.; Hansen, EH. Flow injection analysis. Wiley; New York: 1981.

Saltzman BE. Colorimetric microdetermination of nitrogen dioxide in the atmosphere. Anal Chem 1954;26:1949–1955.

Seibel K, Schöler L, Schäfer H, Böhm M. A programmable planar electroosmotic micropump for lab-on-chip application 2008;18(2):025008/1–025008/7.

Smoluchowski MV. Versuch einer mathematischen theorie der koagulationskinetik kolloider lösungen. Z Phys Chem 1917;92:129–168.

Studer V, Pepin A, Chen Y, Ajdari A. An integrated AC electrokinetic pump in a microfluidic loop for fast and tunable flow control. Analyst 2004;129(10):944–949. [PubMed: 15457328]

Takamura Y, Onoda H, Inokuchi H, Adachi S, Oki A, Horiike Y. Low-voltage electroosmosis pump and its application to on-chip linear stepping pneumatic pressure source. Micro total analysis systems 2001:230–232.

Takamura Y, Onoda H, Inokuchi H, Adachi S, Oki A, Horiike Y. Low-voltage electroosmosis pump for stand-alone microfluidics devices. Electrophoresis 2003;24(1–2):185–192. [PubMed: 12652590]

Tanaka N, Kobayashi H, Ishizuka N, Minakuchi H, Nakanishi K, Hosoya K, Ikegami T. Monolithic silica columns for high-efficiency chromatographic separations. J Chromatogr A 2002;965(1–2):35–49. [PubMed: 12236535]

Tripp JA, Svec F, Frechet JMJ, Zeng SL, Mikkelsen JC, Santiago JG. High-pressure electroosmotic pumps based on porous polymer monoliths. Sens Actuat B Chem 2004;99(1):66–73.

Urbanski JP, Thorsen T, Levitan JA, Bazant MZ. Fast AC electro-osmotic micropumps with nonplanar electrodes. Appl Phys Lett 2006;89(14):143508/1–143508/3.

Urbanski JP, Levitan JA, Burch DN, Thorsen T, Bazant MZ. The effect of step height on ac electro-osmotic microfluidic pumps. J Colloid Interf 2007;309(2):332–341.

Wallner JZ, Nagar N, Friedrich CR, Bergstrom PL. Macro porous silicon as pump media for electro-osmotic pump. Phys Stat Sol (a) 2007;204(5):1327–1331.

Wang P, Chen ZL, Chang HC. A new electro-osmotic pump based on silica monoliths. Sens Actuat B Chem 2006;113(1):500–509.

Wu J. Ac electro-osmotic micropump by asymmetric electrode polarization. J Appl Phys 2008;103(2):024907/1–024907/5.

Xie C, Hu J, Xiao H, Su X, Dong J, Tian R, He Z, Zou H. Electrochromatographic evaluation of a silica monolith capillary column for separation of basic pharmaceuticals. Electrophoresis 2005;26(4–5):790–797. [PubMed: 15714568]

Yang L, He YZ, Gan WE, Li M, Qu QS, Lin XQ. Determination of chromium(VI) and lead(II) in drinking water by electrokinetic flow analysis system and graphite furnace atomic absorption spectrometry. Talanta 2001;55(2):271–279. [PubMed: 18968370]

Yao, S.; Huber, D.; Mikkelsen, JC.; Santiago, JG. A large flowrate electroosmotic pump with micron pores. Proceedings of the international mechanical engineering congress and exposition, sixth microfluids symposium; New York. 2001. p. 1-7.

Yao S, Hertzog DE, Zeng S, Mikkelsen JC, Santiago JG. Porous glass electroosmotic pumps: design and experiments. J Colloid Interf Sci 2003;268(1):143–153.

Yao S, Myers AM, Posner JD, Rose KA, Santiago JG. Electroosmotic pumps fabricated from porous silicon membranes. J Microelectromech Syst 2006;15(3):717–728.

Zeng S, Chen CH, Mikkelsen JC, Santiago JG. Fabrication and characterization of electroosmotic micropumps. Sens Actuat B Chem 2001;79(2–3):107–114.

Zeng S, Chen CH, Santiago JG, Chen J, Zare RN, Tripp JA, Svec F, Frechet J. Electroosmotic flow pumps with polymer frits. Sens Actuat B 2002;82(2–3):209–212.

Zhao YQ, He YZ, Gan WE, Yang L. Determination of nitrite by sequential injection analysis using electrokinetic flow analysis system. Talanta 2002;6(4):619–625. [PubMed: 18968536]

Zou HF, Huang XD, Ye ML, Luo QZ. Monolithic stationary phases for liquid chromatography and capillary electrochromatography. J Chromatogr A 2002;954(1):5–32. [PubMed: 12058917]
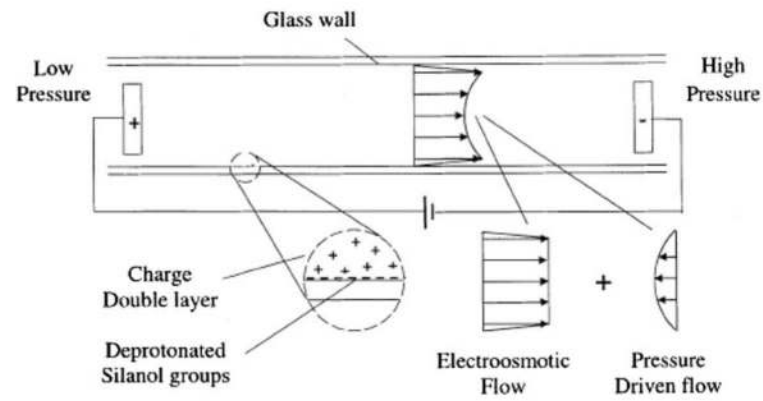
Fig. 1.
Schematic illustration of electric double layer and principle of EO flow. In EOF, mobile ions in the diffuse counter-ion layer of the electric double layer are driven by an externally applied electrical field. These moving ions drag along bulk liquid through viscous force interaction. The net flow is the superposition of EOF and pressure forces. Reprinted with permission from Chen and Santiago 2002
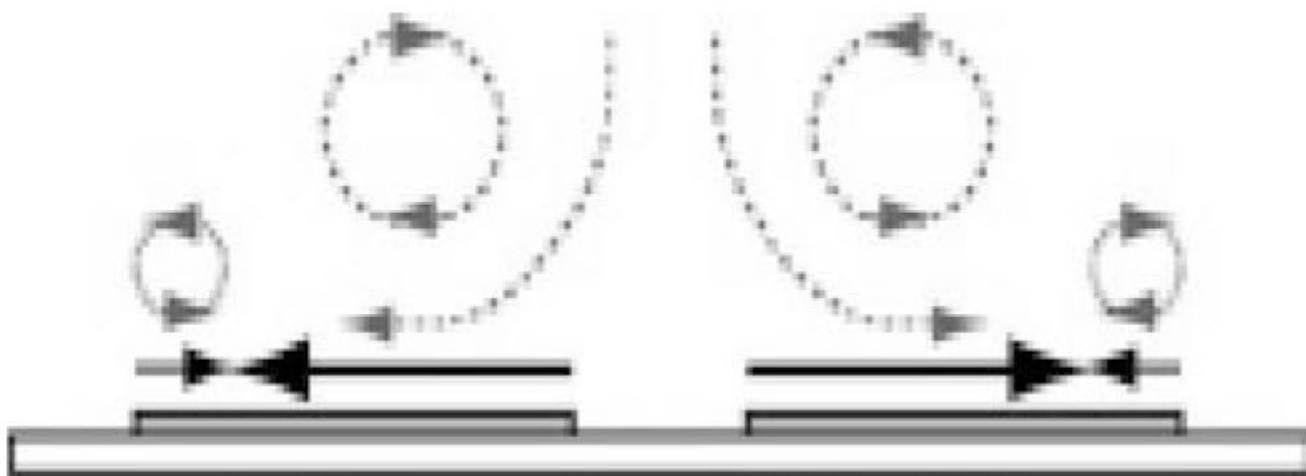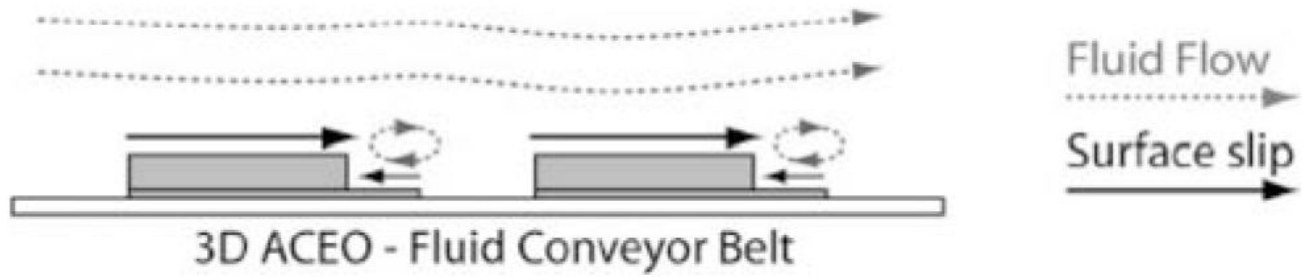
Fig. 2.
Schematic diagram of AC electroosmotic flow in a symmetric electrode array. Surface slip at electrodes, and resulting fluid streamlines are represented with *solid* and *broken lines*, respectively. Reprinted with permission from Urbanski et al. 2006
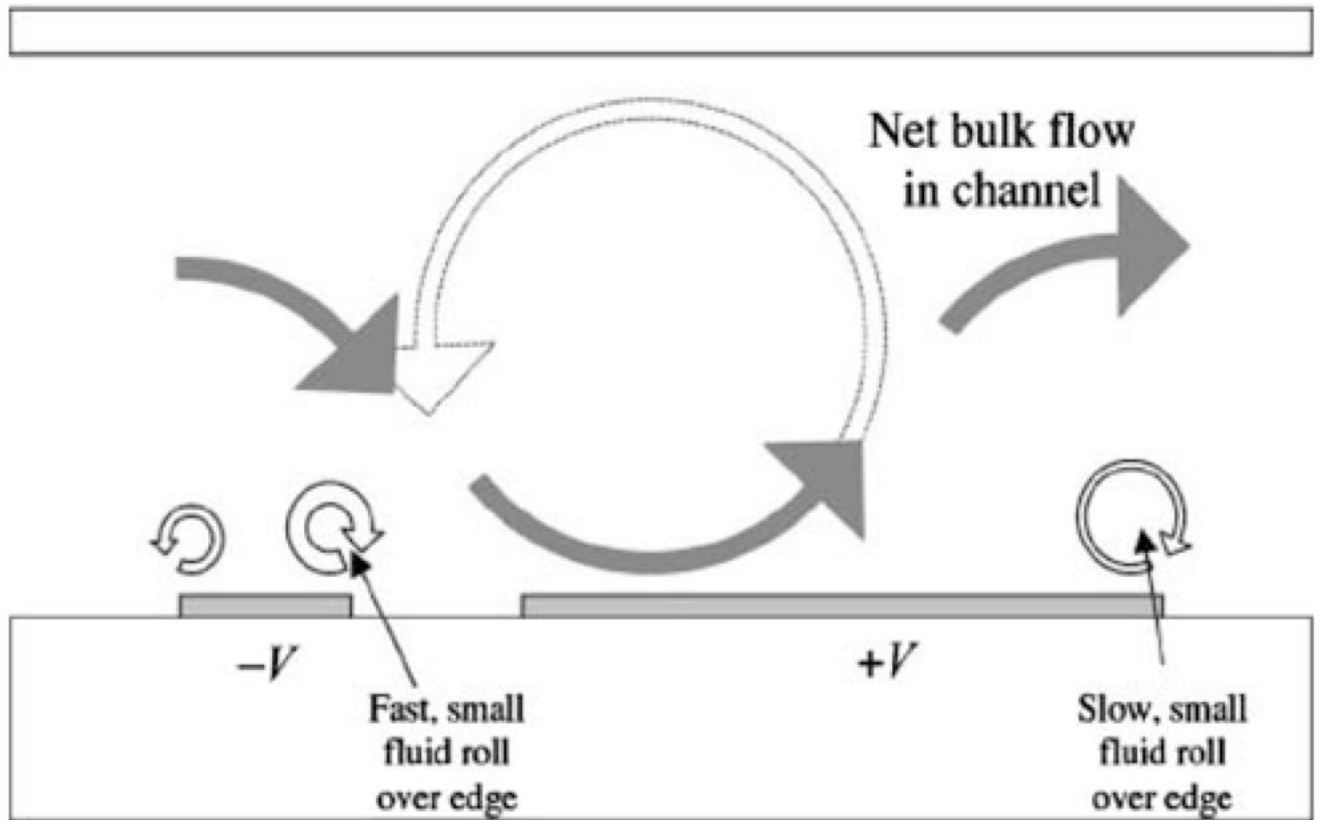
Fig. 3.
Schematic diagram of AC electroosmotic flow in an asymmetric electrode array. The asymmetry leads to fluid rolls of different sizes over each electrode resulting in a net fluid flow. Reprinted with permission from Ramos et al. 2003

Fig. 4.
Schematic diagram of AC electroosmotic flow in a 3D stepped electrode array. Surface slip at electrodes, and resulting fluid streamlines are represented with *solid* and *broken lines*, respectively. Reprinted with permission from Urbanski et al. 2006
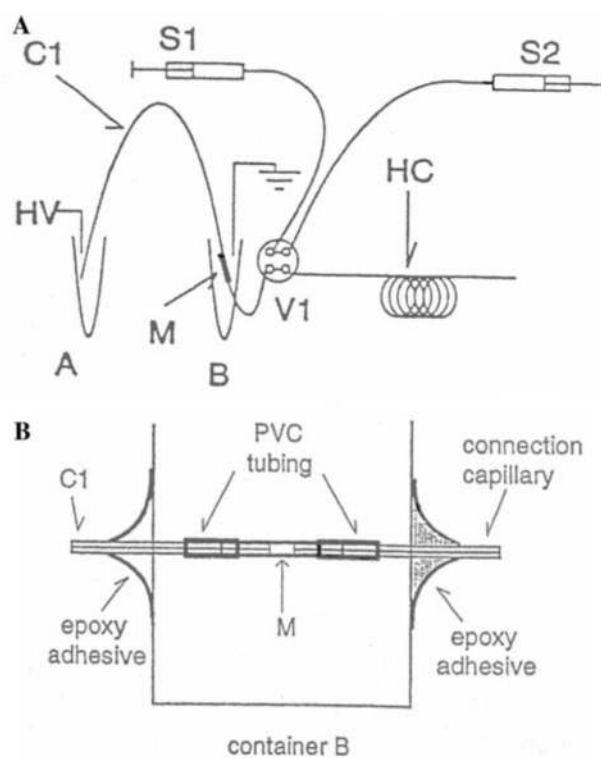
Fig. 5.
Schematic diagram of an stand-alone EOP: **a** schematic configuration of an stand-alone EOP; **b** detailed structure of a membrane joint. *A* Pump electrolyte container; *B* vial housing *M* and containing the same solution as *A*; *HV* high-voltage power supply; *C1* pumping capillary; *M* membrane; *V1* four-way valve; *S1* and *S2* syringes respectively holding pump buffer solution and reagent solutions; *HC* reagent holding coil. Reprinted with permission from Dasgupta and Liu 1994
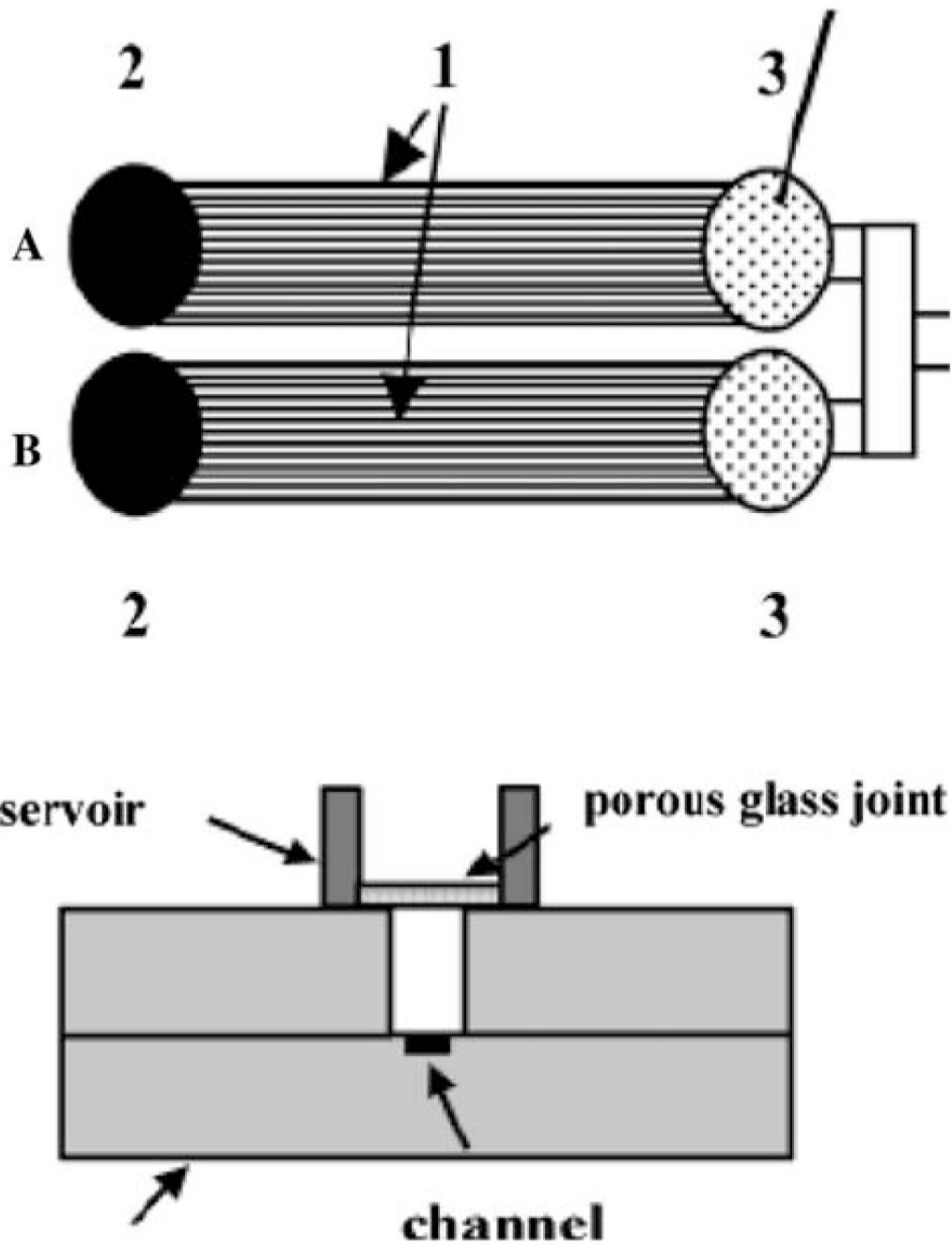
Fig. 6.
Open-channel EOP. *1* Open-channel EOP, *2* micropump inlet reservoir, and *3* micropump outlet reservoir. The *bottom figure* shows an expanded view of reservoir 3 containing the porous glass disk. Reprinted with permission from Lazar and Karger 2002
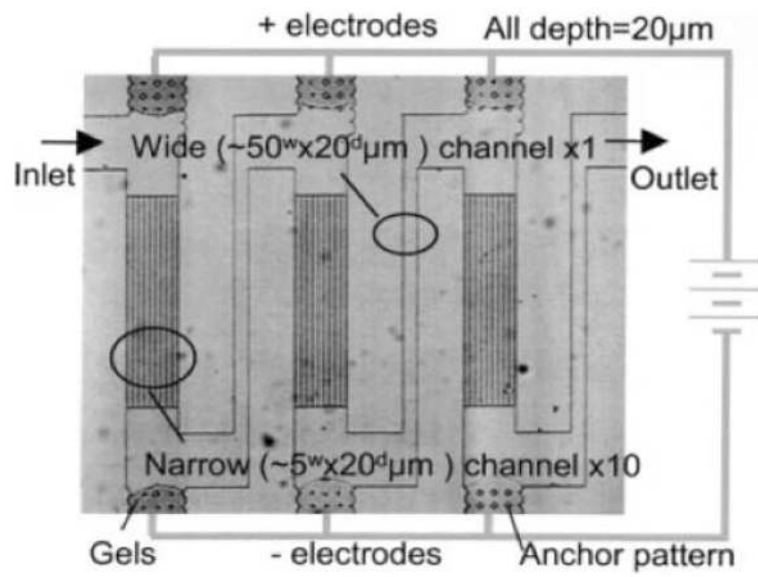
Fig. 7.
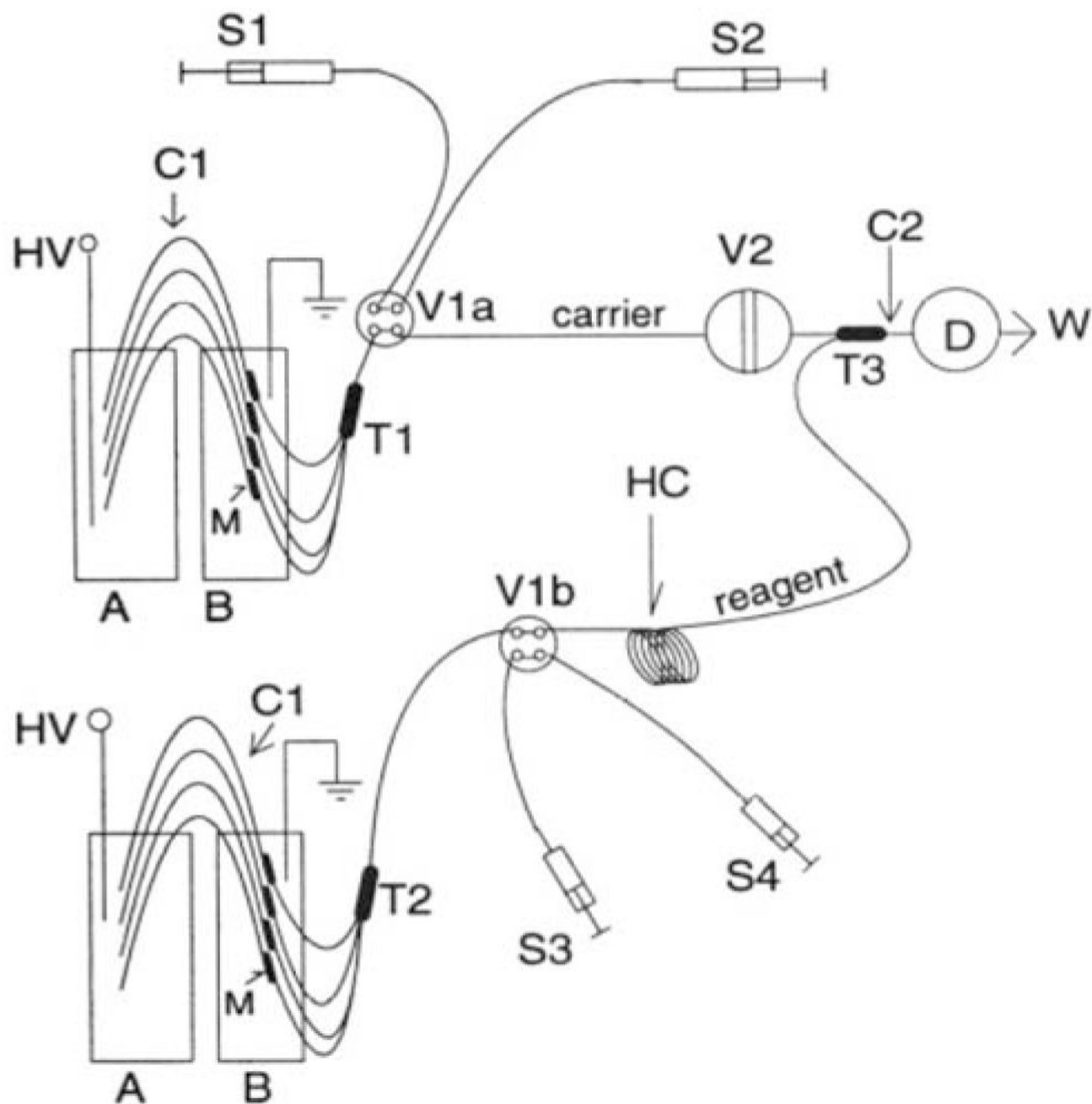Photograph of fabricated cascade-type EOP. Reprinted with permission from Takamura et al. 2003

Fig. 8.
Schematic diagram of two-line FIA system with EOF pumping: B, pump electrolyte solution container; T1, T2, capillary unions; Vla and Vlb, four-way valve stacks a and b; S1 and S3, syringes holding pump buffer solution; S2 and S4, syringes respectively holding carrier and reagent solutions; HC, reagent holding coil; T3, low-volume tee union. Reprinted with permission from Dasgupta and Liu 1994
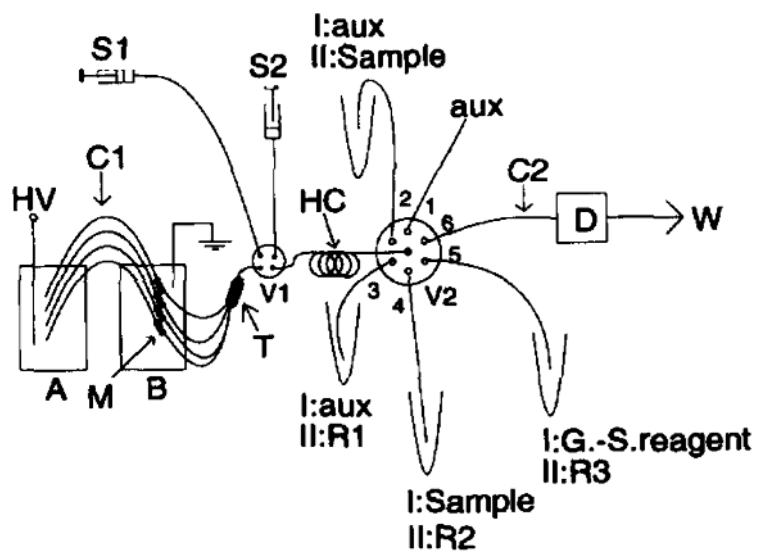
Fig. 9.
Schematic diagram of capillary format SIA system. *HV* High-voltage power supply; *A*, *B* pumping electrolyte solution containers; *M* membrane joint; *C1* pumping capillary; *T* 4 × 1 union; *HC* holding coil; *V1* four-way valve; *S1*, *S2* syringes; *V2* 6 × 1 selector valve; *R1*, *R2*, *R3* reagents; aux, unused auxiliary solution port. Reprinted with permission from Liu and Dasgupta 1994
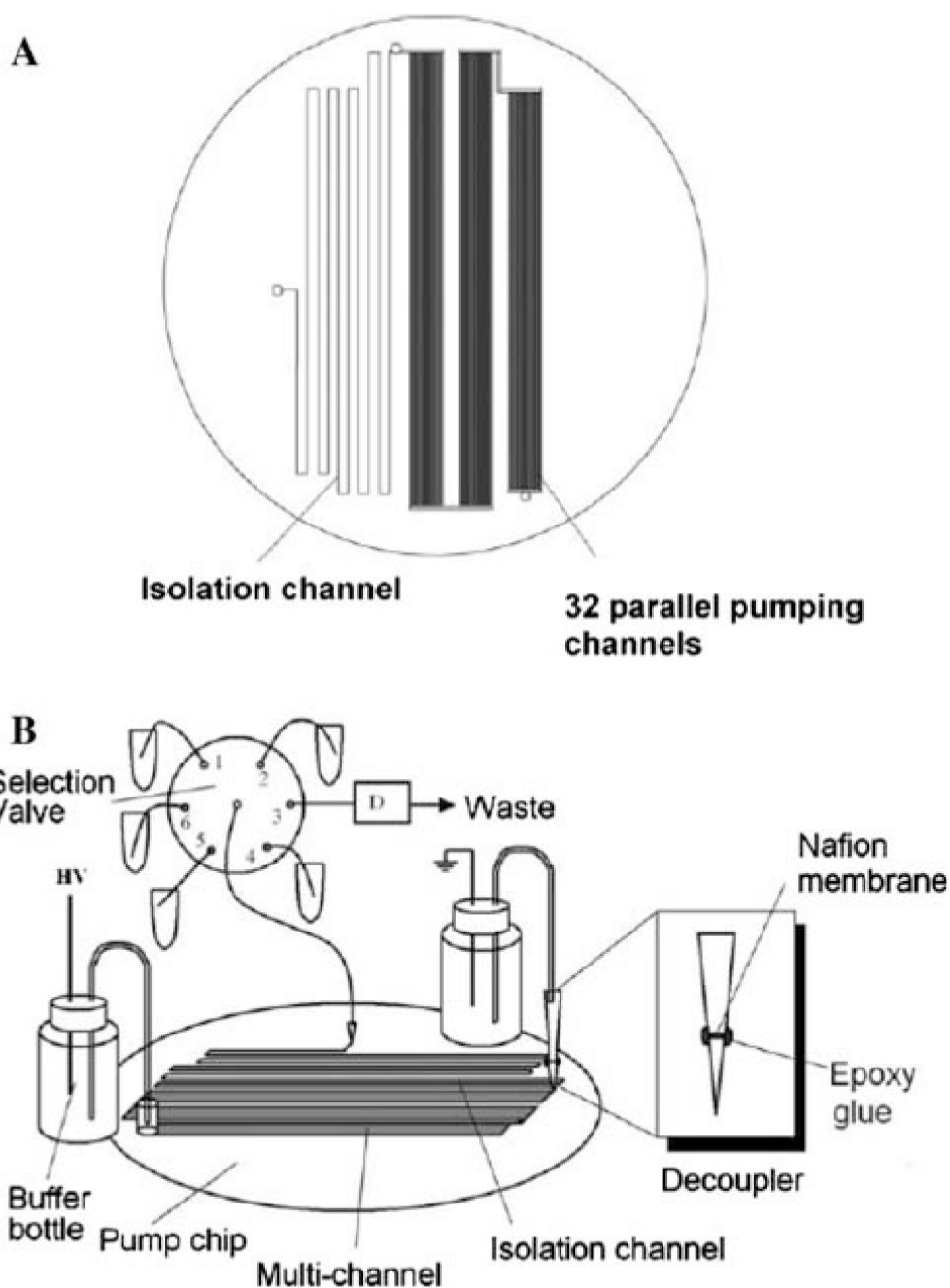
Fig. 10.
a The photomask design of the pump chip. **b** Schematic arrangement of the micro-EOP-SIA system. Reprinted with permission from Pu and Liu 2004
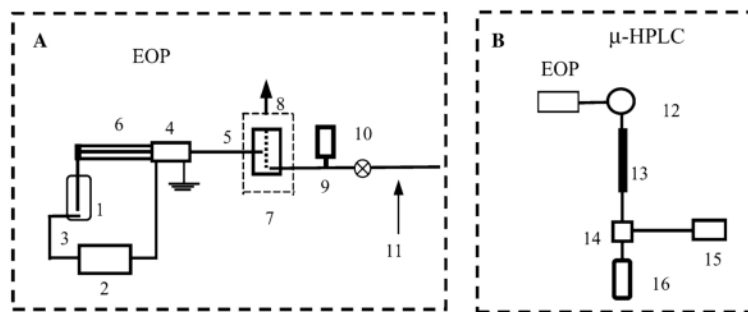
Fig. 11.
Schematic diagram of the one-stage EOP and the μ-HPLC system. **a** The EOP system: *1* solvent reservoir, covered with an insulating sheath; *2* high-voltage direct current source module; *3* Pt wire; *4* hollow electrode (grounded); *5* capillary conduit; *6* packed columns, three packed columns connected in parallel; *7* gas releasing device (*8* representation of gas leaving direction); *9* liquid pressure sensor; *10* open/close valve; *11* measurement point of flow rate. **b** The μ-HPLC system: *12* a four-port injection valve; *13* analytical capillary HPLC column; *14* an on-column UV—Vis detector; *15* chromatographic data station; *16* waste liquid bottle. Reprinted with permission from Chen et al. 2004
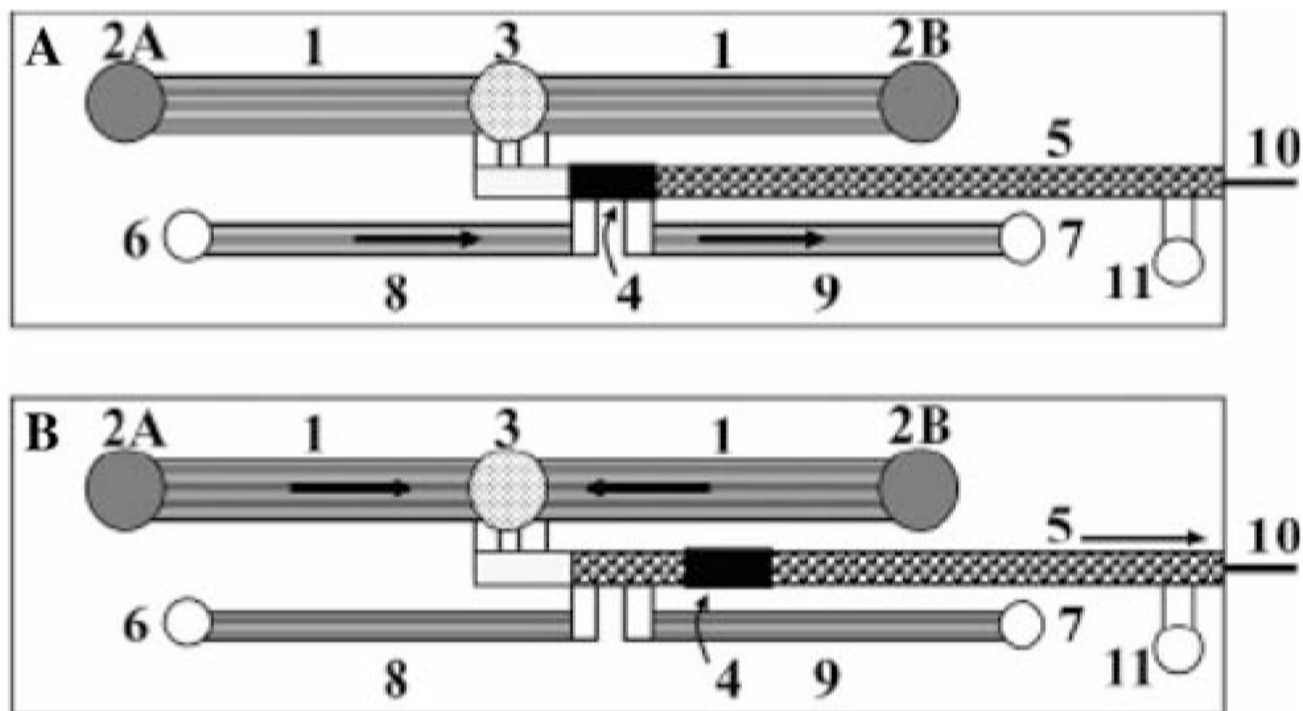
Fig. 12.
Schematic representation of a microfluidic LC system. *1* Pumping channels; *2A*, *2B* eluent inlet reservoirs; *3* eluent outlet reservoir; *4* double-T injector that contains the sample plug; *5* separation channel; *6* sample reservoir; *7* sample waste reservoir; *8* sample inlet channels; *9* sample outlet channels; *10* ESI capillary emitter; *11* LC waste reservoir. **a** Sample loading; **b** sample analysis. *Arrows* indicate the main flow pattern through the system. Reprinted with permission from Lazar et al. 2006

Table 1

Summary of the the performance metrics reported for the various EOPs

Type of EOPs	Structure	Pumping solution	Applied voltage	Flow rates	Pumping pressure	Application	References
Open-channel EOPs	Two nanopumps made of six 83-mm long, 300-µm wide and 50-µm deep microchannels connected in parallel	10 mM borax	1 kV	1.25 µL/min		Volumetric nanotitrations	Guenat et al. 2001
	A 1-mm wide, 100-µm long and 120-nm deep channel	1/10 phosphate buffer	40 V		5 kPa		Takamura et al. 2001
	A wide, short and shallow (38 mm × 1 mm × 0.9 µm) pump channel, incorporated with eight equally distributed 0.25-mm wide ribs	DI water	1 kV	15 µL/min	33.4 kPa		Chen and Santiago 2002
	1–100 pumping channels with 1–6 µm deep and 4–50 mm long	Buffer solution (15.4 mM NH4HCO3/CH3OH)	2 kV	10–400 nL/min	551.3 kPa	Deliver samples for ESI-MS	Lazar and Karger 2002
	A single channel with 400 nm deep, 85 µm long and 33.2 mm wide folded 39 times	1/10 phosphate buffer	10 V	415 nL/min	0.8 kPa		Takamura et al. 2003
	10 stage cascade EOP consist of 130-nm deep channels and 20-µm deep channels	1/10 phosphate buffer	10 V		25 kPa		Takamura et al. 2003
	100–1,000 parallel microchannels (7–10 µm wide, 5–20 mm long and 1.5 ~ 1.8 µm deep)	15 mM NH4HCO3 in H2O/CH3OH at pH ~ 8	500 V/cm	10–400 nL/min	689.1– 1378.2 kPa	µ-LC—MS	Lazar et al. 2006
	A single channel (50 µm wide and 5 mm long) with multiple pump arms (5 µm wide and 4 mm long)	10 mM carbonate buffer at pH 9.2	4–400 V	0.19–2.30 µL/ min			Edwards IV et al. 2007
	"Y" shape pumping channel designed with two arms (40 µm wide, 30 µm deep and 12.6 mm long) with positively and negatively charged interior surface, respectively. And a field-free channel was 10 mm long	10 mM phosphate buffer at pH 7.0	1.0 kV/cm	262.4 nL/min			Joo et al. 2007
	A programmable planar electroosmotic micropump consisting of an arrangement of multiple vertical narrow gap microchannels	DI water	40 V	10 nL/min	65 Pa		Seibel et al. 2008

Type of EOPs	Structure	Pumping solution	Applied voltage	Flow rates	Pumping pressure	Application	References
Packed-column EOPs	530 μm i.d. and 54 mm long capillary packed with 3.5 μm non-porous silica particles	DI water	2 kV	4.8 lL/min	2381.1 kPa		Zeng et al. 2001
	Pumping chamber was filled with packed non-porous silica particles and held in place using two polymeric porous frits	DI water	1.0 kV	0.8 mL/min	202.7 kPa		Zeng et al. 2002
	360 μm o.d. and 100 or 150 μm i.d. capillaries packed with 1 or 5 μm diameter nonporous silica microspheres	10 mM Tris buffers added with zwitterionic additive		0.27 μL/min per kV	156 kPa/V		Reichmuth and Kirby 2003
	Two 500-μm channels, one packed with anion exchange beads and the other packed with cation exchange beads	25 mM phosphate buffer at pH 6.8	3 kV	2 μL/min			Razunguzwa and Timperman 2004
	Three 20 cm × 530 μm i.d. capillaries packed with 20 ± 5 nm silica grains	3.0 mM sodium dihydrogenphosphate buffer at pH 7.5	10 kV	6.4 μL/min	20 MPa	Capillary LC	Chen et al. 2005a
		Methanol	10 kV	4.5 μL/min	28 MPa		
		Methanol-phosphate buffer	10 kV	5.7 μL/min	33 MPa		
	Three-stage 10 cm × 320 μm i.d. capillary packed with 2 μm porous silica particles	2 mM sodium dihydrogen phosphate buffer at pH 7.5	5 kV	1.7 μL/min	12.5 MPa		Chen et al. 2005b
	A straight channel (3 cm × 160 μm × 62 μm) packed with porous silica microspheres held by a weir	10 mM cyclohexylamino alkyl sulfonate CHES	3,500 V	85 nL/min	2.533 kPa		Borowsky et al. 2008b
	A straight channel (3 cm × 230 μm × 100 μm) packed with porous silica beads held by a weir	Tris/acetonitrile	2,000–5,000 V			μ-HPLC	Borowsky et al. 2008b
Porous-membrane EOPs	Porous boric glass core with 35 mm in diameter, 13 mm thick and 2–5 μm i.d. pore size	0.35 mM NH4OH	500 V	3.0 mL/min	0.15 MPa	FIA	Gan et al. 2000
	Porous sintered-glass frit with 30 mm in diameter and 1.5–3 mm thick	1 mM borate buffer	200 V	7 mL/min	253.3 kPa		Yao et al. 2001
	A porous glass filter disk with a diameter of 30 mm and a thickness of 2 mm and an effective pore diameter of 1 μm	1 mM borax buffer	200 V	7 mL/min	160 kPa	Microchannel cooling system	Jiang et al. 2002
	Porous sintered-glass frit with 40 mm in diameter, 1–5 mm	1 mM borate buffer at pH 9.2	100 V	33 mL/min	131.7 kPa		Yao et al. 2003

NIH-PA Author Manuscript

Type of EOPs	Structure	Pumping solution	Applied voltage	Flow rates	Pumping pressure	Application	References
	thick and 1 μm pore size						
	140-μm anion exchange membrane	5 mM borate buffer	30 V	6 μL/min	450 kPa		Brask et al. 2005
	Porous silicon membranes	1 mM borate buffer	25 V	3.2 mL/min	~0.72 kPa		Yao et al. 2006
	Ten-stage membrane	1 mM electrolyte solution	370 V	0.17 mL/s	1.6 MPa		Prakash et al. 2006
	Macro porous silicon membrane	DI water	60 V	11.9 μL/min	5.2 kPa		Wallner et al. 2007
	Aluminum oxide membranes with silica coating	DI water	70 V	86 mL/cm² per min			Miao et al. 2007
	Porous anodic alumina membranes	10^{-6} M KCl	20 V	0.09 mL/min per V/cm²			Chen et al. 2008c
	Porous silica disk with a length of 3.5 mm, a porosity of 35%, and a pore radius of 0.75 μm	DI water	150 V	13.6 mL/min	2 kPa		Berrouche et al. 2008
Porous monolith EOPs	Polymer monolithic disks grafted ionizable functionalities	0.5 M borate buffer at pH 9.2	50 V	0.41 ml/min	0.38 MPa		Tripp et al. 2004
	A 100 μm i.d. and 6 cm long monolithic silica column	0.26 mM Tris-1.5 mM EDTA buffer at pH 6.0	6 kV	0.4 μL/min	0.4 MPa	μ-FIA	Chen et al. 2005c
	A 100 μm i.d. and 6 cm long monolithic silica column with ~4 μm pores size	DI water	6 kV	2.9 μL/min	304.0 kPa		Wang et al. 2006
	Triple 10 × 0.1 mm i.d. monolithic silica columns	2 mM acetate buffer at pH 4.5	2 kV	0.1 μL/min	240 kPa		Nie et al. 2007a
	Monolithic silica column	2 mM sodium chloride	2 kV	400 nL/min		μ-FIA	Nie et al. 2007b
ACEOPs	An interdigitated electrode array consisting of 130 pairs of electrodes (100-nm Au/10-nm Nichrome) with alternating widths of 4.2 μm and 25.7 μm separated by 4.5 μm (edge-to-edge)	0.1 mM NaNO₃	1.2 V_{rms}	75 μm/s			Brown et al. 2001
	An array of 564-pair circular electrodes (70-nm Au/5-nm Cr), each pair consisting of a 4 μm wide electrode, a 5 μm wide gap, a 26 μm wide electrode and a 16 μm wide gap	0.1 mM KNO₃	1 V_{rms} (at 5 kHz)	50 μm/s			Debesset et al. 2004
	An array of 16 pairs of electrodes, each pair consisting of two 100 μm wide and 1000 μm long Al electrodes orthogonally	NaCl solution	20 V_{rms}	>1 mm/s			Lastochkin et al. 2004

Type of EOPs	Structure	Pumping solution	Applied voltage	Flow rates	Pumping pressure	Application	References
	arranged in a T-shape with a gap of 150–500 μm between the electrodes						
	An array of electrodes with alternating heights (15 μm and 2.7 μm), all electrodes having a width of 20 μm and a 5 μm gap between adjacent electrodes	Deionized water	2 V_{rms} (at 1 kHz)	420 μm/s			Urbanski et al. 2006